Zoledronic acid enhances tumor growth and metastatic spread in a mouse model of jaw osteosarcoma

Than-thuy Nham, Romain Guiho, Régis Brion, Jérôme Amiaud, Bénédicte Brounais Le Royer, Anne Gomez-brouchet, Françoise Rédini, Hélios Bertin

Received: 21 October 2023 | Revised: 8 January 2024 | Accepted: 6 February 2024

DOI: 10.1111/odi.14897

ORAL DISEASES Leading in Oral, Maxillofacial, Head & Neck Medicine WILEY

ORIGINAL ARTICLE

Zoledronic acid enhances tumor growth and metastatic spread in a mouse model of jaw osteosarcoma

Than-Thuy Nham[1,2] | Romain Guiho[3] | Régis Brion[2] | Jérôme Amiaud[2] | Bénédicte Brounais Le Royer[2] | Anne Gomez-Brouchet[4,5] | Françoise Rédini[2] | Hélios Bertin[1,2]

[1]Nantes Université, CHU Nantes, Service de Chirurgie Maxillo-Faciale et Stomatologie, Nantes, France

[2]Nantes Université, Univ Angers, CHU Nantes, INSERM, CNRS, CRCI2NA, Nantes, France

[3]Nantes Université, Oniris, Univ Angers, CHU Nantes, INSERM, Regenerative Medicine and Skeleton, RMeS, UMR 1229, Nantes, France

[4]Cancer Biobank of Toulouse, IUCT Oncopole, Toulouse University Hospital, Toulouse Cedex 9, France

[5]Department of Pathology, IUCT Oncopole, Toulouse University Hospital, Toulouse Cedex 9, France

Correspondence
Hélios Bertin, Nantes Université, CHU Nantes, Service de chirurgie maxillo-faciale et stomatologie, F-44000 Nantes, France.
Email: helios.bertin@chu-nantes.fr

Funding information
Centre Hospitalier Universitaire de Nantes; Fondation des Gueules Cassées, Grant/Award Number: 2018-51

Abstract

Objectives: Investigation of the therapeutic effect of zoledronic acid (ZA) in a preclinical model of jaw osteosarcoma (JO).

Materials and Methods: The effect of 100 μg/kg ZA administered twice a week was assessed in a xenogenic mouse model of JO. The clinical (tumor growth, development of lung metastasis), radiological (bone microarchitecture by micro-CT analysis), and molecular and immunohistochemical (TRAP, RANK/RANKL, VEGF, and CD146) parameters were investigated.

Results: Animals receiving ZA exhibited an increased tumor volume compared with nontreated animals ($71.3 \pm 14.3\,mm^3$ vs. $51.9 \pm 19.9\,mm^3$ at D14, respectively; $p = 0.06$) as well as increased numbers of lung metastases (mean 4.88 ± 4.45 vs. 0.50 ± 1.07 metastases, respectively; $p = 0.02$). ZA protected mandibular bone against tumor osteolysis (mean bone volume of $12.81 \pm 0.53\,mm^3$ in the ZA group vs. $11.55 \pm 1.18\,mm^3$ in the control group; $p = 0.01$). ZA induced a nonsignificant decrease in mRNA expression of the osteoclastic marker TRAP and an increase in RANK/RANKL bone remodeling markers.

Conclusion: The use of bisphosphonates in the therapeutic strategy for JO should be further explored, as should the role of bone resorption in the pathophysiology of the disease.

KEYWORDS
bisphosphonates, bone resorption, mandible, osteosarcoma, tumor microenvironment

1 | INTRODUCTION

Osteosarcoma is the most common type of malignant bone tumor. Most of the cases are long bone osteosarcomas (LBOs), affecting the bone metaphysis during growth in children and adolescents (Baumhoer et al., 2014). Jaw osteosarcoma (JO) is a rare disease, as it accounts for only 6%–13% of all osteosarcomas and less than 1% of malignant head and neck tumors (Baumhoer et al., 2014; Boon et al., 2017; Krishnamurthy & Palaniappan, 2018; Thariat et al., 2012). There is evidence that JO differs from LBO in many ways (Bertin et al., 2020; Weber et al., 2023). Occurring at an average age of 35 years, JO manifests two decades later than LBO (Kontio et al., 2019; Lee et al., 2015; van den Berg & Merks, 2013). JO also exhibits a lower incidence of lung metastasis, occurring in 14%–17% of patients within 2 years after diagnosis, while 25% of patients with LBO have primary metastases at the time of diagnosis

(Baumhoer et al., 2014; Bertin et al., 2023). Finally, the 5-year survival rate of JO can reach 77% for patients with localized tumors and after complete carcinologic resection, compared with 55% for all osteosarcomas (Granowski-LeCornu et al., 2011; Nissanka et al., 2007; Thariat et al., 2012).

Multimodal treatment is based on neoadjuvant chemotherapy (neo-CT), consisting of the association of high-dose methotrexate with etoposide-ifosfamide (M-EI) in children and adolescents, and doxorubicin-cisplatin-ifosfamide (API-AI) in adult patients (Marec-Berard et al., 2020; Piperno-Neumann et al., 2020). Nevertheless, the benefit of neo-CT is a subject of controversy in JO, as it is not associated with a survival benefit and it can delay surgical treatment leading to nonoperable patients (Bouaoud et al., 2019; Khadembaschi et al., 2022). New treatment strategies propose direct radical surgery when resection with healthy margins (R0) can be achieved (Khadembaschi et al., 2022; Weber et al., 2023). R0 resection represents the main prognostic factor for local control and survival (Lee et al., 2015; Thariat et al., 2012, 2013; Weber et al., 2023). The adjuvant chemotherapy is tailored according to the histological response on the tumor resection, as assessed by the Huvos and Rosen score (Crenn et al., 2017; Gomez-Brouchet et al., 2019). The use of external radiotherapy is also controversial, and it is reserved for inoperable or incompletely resected patients (Bialick et al., 2023; Seidensaal et al., 2022; Weber et al., 2023). Despite the efforts of researchers, patient survival has not improved over the past four decades, and there is an urgent need to develop new therapeutic strategies (Piperno-Neumann et al., 2020; Zhu et al., 2022).

Osteosarcoma is a tumor of mesenchymal origin characterized by the proliferation of osteoblastic precursors and the production of osteoid matrix comprised of immature bone. However, the etiology of the disease remains largely unknown. There is a lack of recurrent alterations, and osteosarcoma exhibits an exceptional rate of mutations and genomic alterations (Mirabello et al., 2020; Scotlandi et al., 2020). The tumor microenvironment (TME) has become a potential therapeutic target, as it plays a major role in the development, progression, and chemoresistance of the disease (Alfranca et al., 2015; Heymann et al., 2019; Wu & Dai, 2017; Yu et al., 2022). The specific TME of JO has been studied little to date, but it is likely that there are significant differences between the TME of JO and that of LBO that may explain the differences in the clinical and therapeutic behaviors (Bertin et al., 2020). In a recent immunohistochemical study performed with tissue micro-arrays (TMA) of 50 JO biopsy samples, we highlighted a significant association between the receptor activator of NF-κB (RANK) and the ligand RANKL staining (≥10%) and lower disease-free survival (DFS) in patients ($p_1 = 0.03$ and $p_2 = 0.03$, respectively) (Bertin et al., 2023). The same markers were not correlated with the local relapse and the metastasis spread (data not shown). Conversely, Navet et al. (2018) showed that RANKL expression was significantly lower in metastatic disease based on an immunohistochemical study of 50 patients with LBO. Targeting bone resorption with bisphosphonates or denosumab, a monoclonal antibody against RANKL, is commonly used in case of osteolytic bone metastasis of solid cancers including prostate, breast, and lung cancers (Boopathi et al., 2022; Ishikawa, 2023; Li et al., 2022). In osteosarcoma, the dysregulation of local bone remodeling in favor of osteolysis plays a major role in cancer cell proliferation and migration, as bone degradation releases various factors favorable to tumor progression including transforming growth factor (TGF)-β (Cappariello & Rucci, 2019; Verrecchia & Rédini, 2018). In this context, zoledronic acid (ZA) has been tested in rodent models of LBO, showing a reduction in tumor growth and, to a lesser extent, in metastatic spread (Heymann, Fortun, et al., 2005; Ory et al., 2005). In humans, ZA was tested as an adjunct to chemotherapy in a French phase III trial (OS2006); however, the study had to be stopped prematurely due to the occurrence of metastases and poor prognosis in patients treated with ZA (Piperno-Neumann et al., 2016). The effect of bisphosphonates in JO has not been tested to date. Various syngeneic, xenogenic, and patient-derived xenograft models (PDX) of JO were previously described in mice (Bertin et al., 2019). These models can be used to investigate the TME and to perform targeted therapy studies.

Considering that JO and LBO constitute two different clinical entities and possibly different environments regarding osteolysis, the objective of this study was to investigate the effect of ZA on a murine model of JO.

2 | MATERIALS AND METHODS

2.1 | Cell culture

The human HOS1544 osteosarcoma cell line was purchased from the American Type Culture Collection (ATCC, LGC Promochem, Molsheim, France) and cultured in Dulbecco's Modified Eagle's Medium (DMEM, Lonza, Switzerland) in a humidified 5% CO_2/air atmosphere at 37°C.

2.2 | Animal model

Four-week-old NMRI-nude female mice (Elevages Janvier, France) were housed under pathogen-free conditions at the Experimental Therapy Unit (Medicine School, Nantes, France) in accordance with French institutional guidelines (CEEA.PdL.06, authorization no 8405 and 8449). The mice were provided access to food and water ad libitum. This report adheres to the EU directive 2010/63/EU and the ARRIVE Guidelines for reporting animal research (Percie du Sert et al., 2020), and a completed checklist is included in the Complementary Materials.

The method for obtaining murine models of JO has been described previously (Bertin et al., 2019). Briefly, 0.25×10^6 human osteosarcoma HOS1544 cells suspended in PBS (20 μL) were inoculated in NMRI-nude mice. The tumor induction was performed under general anesthesia (isoflurane-air mixture, 1.5%, 1 L/min), close to the left mandible after periosteum scraping.

After tumors appeared at the graft sites, the mice were randomly assigned to the control or treatment group, with treatment beginning on day 3. The animals in the control group were subcutaneously injected with isotonic sodium chloride solution (50 µL) twice a week. In the ZA group, the animals were subcutaneously injected with 100 µg/kg of ZA (50 µL), kindly provided as the disodium salt by Pharma Novartis AG (Basel, Switzerland), twice a week. The tumor volumes were measured twice a week and calculated using the formula $(l^2 \times L)/2$, where l is the smallest and L is the largest perpendicular diameter of the tumor. The experimental protocol is outlined in Figure 1.

For ethical considerations, the mice were euthanized by cervical dislocation when the tumor volume reached 200 mm^3, and micro-computed tomography (micro-CT) imaging was performed at necropsy. A tumor biopsy was performed at the bone–tumor interface and frozen for molecular analysis, and the head and lungs were then harvested and fixed in 10% buffered formaldehyde for 48 h. The lungs were embedded in paraffin to investigate lung metastases, the heads were decalcified with 4% of ethylenediaminetetraacetic acid (EDTA) and 0.2% paraformaldehyde (PFA) in PBS using a microwave tissue processor (KOS, Milestone, Kalamazoo, MI, USA) for 10 days and then embedded in paraffin.

2.3 | Micro-CT analysis

Mandibles were scanned using a SkyScan-1072 X-ray microcomputed tomography system (Bruker, Massachusetts, USA) with the following parameters: 18 µm pixel size, 50 kV, 0.5 mm Al filter, and a rotation step of 0.7 degrees. Three-dimensional (3D) reconstructions and analysis were performed using NRecon, CTVox, and CTAn 32-bit software (SkyScan). The region of interest (ROI) for measurement of bone microarchitectural variables was defined in the tumor area from the posterior side of the central incisor over a length of 4.7 mm, as previously described (Bertin et al., 2019). The following parameters were calculated on 3D images (Bouxsein et al., 2010):

- Cortical bone morphology: bone volume (BV) corresponding to the volume of the mandibular cortical bone, and the BV fraction (BV/TV) corresponding to the ratio of the segmented BV to the total volume of the ROI.
- Bone microarchitecture: trabecular thickness (Tb.Th), trabecular separation, and trabecular number (Tb.N).

2.4 | Quantitative reverse transcription-polymerase chain reaction (RT-PCR) analysis

Total RNA was extracted from tumors using TRIzol® reagent (Invitrogen, Carlsbad, USA). The RNA quantity and quality were evaluated by determining the A260/A280 ratio using a NanoDrop® ND-1000 (ThermoFisher Scientific, Waltham, USA). Reverse transcription was performed from 1 µg of isolated RNA using ThermoScript™ RT-PCR System (Invitrogen). Quantitative PCRs were carried out on a CFX96™ Real-Time PCR Detection System (Bio-Rad) using primers (Table 1) and SYBR® Green SuperMix reagents (Applied Biosystems, Waltham, USA). Target gene expression was normalized to human *hGAPDH* and *mHPRT* levels in respective samples as an internal standard, and the comparative cycle threshold method was used to calculate the relative quantification of the target mRNAs. Each assay was performed in triplicate. Both human (i.e., secreted by the tumor in this xenogenic model) and murine (secreted by the host) markers were investigated to assess the mechanisms involved in bone resorption and vascularization.

2.5 | Histologic and immunohistochemical analysis

For analysis of metastasis, 3-µm-thick sections of the lungs were generated every 300 µm, and the tumor foci were quantified using NDP.view2 Hamamatsu software (SZK, Japan).

Immunohistochemical stainings were performed on 3 µm sections of tumor samples. After automated deparaffinization, sections were pretreated with Tris-EDTA pH 9 (EZ Prep solution, Ventana Medical Systems, Arizona, USA) at 69°C for 20 min for CD146, in citrate buffer (Ventana) pH 6 for 20 min for the markers RANKL/RANK. Endogenous peroxidase activity was blocked by 3% hydrogen peroxide for 15 min. The samples were then incubated with primary antibody directed against RANKL (1/25, sc-7628, Santa-Cruz, Heidelberg, Germany), RANK (1/25, sc-9072, Santa-Cruz), and CD146 (1/400, ab75769, Abcam, Cambridge, UK). Immunodetection was performed using secondary

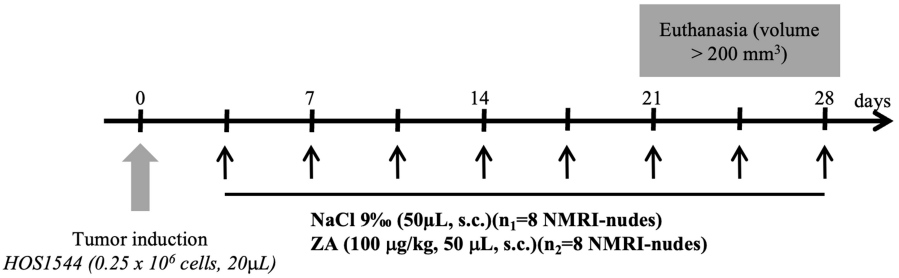

FIGURE 1 Experimental protocol for treating animals with saline solution (NaCl) or zoledronic acid (ZA) twice a week (black arrows). s.c., subcutaneous.

TABLE 1 Primer sequences used in the quantitative real-time PCR analysis.

Gene	Forward primer	Reverse primer
hTRAP	AAGACTCACTGGGTGGCTTTG	GGCAGTCATGGGAGTTCAGG
mTRAP	CGTCTCTGCACAGATTGCAT	AAGCGCAAACGGTAGTAAGG
hRANKL	GTTGGCCGCAGACAAGAA	CGCAGGTACTTGGTGTAGTCTCT
mRANKL	GCAGAAGGAACTGCAACACA	GATGGTGAGGTGTGCAAATG
hRANK	AGAGACCAGCCCGAGGAT	CTGTTTCCAGTCACATTTCCAG
mRANK	TGCAGCTCTTCCATGACACTG	CAGCCACTACTACCACAGAGATG
hVEGF	CCTTGCTGCTCTACCTCCAC	CCACTTCGTGATGATTCTGC
mVEGF	GTACCTCCACCATGCCAAGT	CTGCATGGTGATGTTGCTCT

biotinylated antibodies, and streptavidin HRP complex was revealed with 3,3′-diaminobenyidine (DAB-Dako) followed by counterstaining with hematoxylin. Negative control was determined using a similar procedure without primary antibody. Histoenzymological analysis of TRAP (Tartrate-resistant acid phosphatase) was used to assess osteoclast activation. Slides were prepared on SuperFrost® Plus EV and then deparaffinized and incubated with TRAP labeling solution for 60 min at 37°C, rinsed with distilled water, counterstained with hematoxylin for 90 s, rinsed again three times, and oven-dried before mounting.

The CD146 marker was quantitatively assessed using ImageJ software (National Institutes of Health, Bethesda, USA) according to the method developed by Schneider et al. (2012). Three to five tiles were selected at the bone–tumor interface, and an ROI was selected to measure the number of vascular elements per mm^2 using a macro obtained by thresholding the color of pixels corresponding to vascular elements. For TRAP, an immunoscore was assigned from 1 to 4 according to the density of the labeled cells at the bone–tumor interface. All the markers were analyzed qualitatively by a pathologist specialized in the analysis of bone tumors (A.G.B.).

2.6 | Statistical analysis

The statistical analysis was performed using GraphPad Prism 9.0 software for Mac (GraphPad Software, La Jolla, CA, USA). A two-factor ANOVA test with a mixed effect model and Sidak's correction was used for the comparison of tumor volumes. Kaplan–Meier survival curves were constructed using a Cox regression model, taking euthanasia of the animal as the event and thus the reaching of a tumor volume of 200 mm^3. Lung metastasis and microarchitectural parameters were compared with a Mann–Whitney or a Wilcoxon test for paired observations. A p-value of less than 0.05 was taken to indicate statistical significance.

3 | RESULTS

3.1 | Effect of ZA on tumor growth and metastatic spread

A palpable tumor developed as early as day 5 (D5), with homogeneous tumor growth over time ($p < 0.0001$, mixed effect model). Two animals in the control group and one animal in the ZA group did not develop mandibular tumors and were excluded from the comparative analysis of tumor volumes. Faster tumor growth was observed in the animals treated with ZA compared with the control group as early as D14 ($71.3 \pm 14.3\ mm^3$ vs. $51.9 \pm 19.9\ mm^3$, respectively; $p = 0.06$), requiring euthanasia of the animals at D21–D23 (Figure 2a). The critical tumor volume was reached between D23 and D30 in the animals treated with placebo (Figure 2b).

Two animals in the control group and six animals in the ZA group developed lung metastasis (mean 0.50 ± 1.07 and 4.88 ± 4.45 metastases, respectively; $p = 0.02$) (Figure 2c,d).

3.2 | Effect of ZA on bone microarchitecture around the tumor

The tumor induced osteolysis of the peri-tumoral cortex, as evidenced by the reduction in the BV in the half-mandible affected by the tumor compared with the contralateral mandible in placebo-treated animals ($11.55 \pm 1.18\ mm^3$ vs. $12.4 \pm 0.68\ mm^3$, respectively; $p = 0.03$) (Figure 3a). Treatment with ZA resulted in an increase in cortical BV around the tumor compared with the animals in the control group ($12.81 \pm 0.53\ mm^3$ vs. $11.55 \pm 1.18\ mm^3$, respectively; $p = 0.01$) (Table 2). This bone protection effect observed with ZA around the tumor was also visible on three-dimensional reconstructions of micro-CTs (Figure 3b). Regarding the cancellous bone, ZA induced a significant improvement in the mean Tb.Th and a decrease in the mean Tb.N (Table 2).

3.3 | Analysis of the resorption and vascularization markers

In order to understand the mechanisms involved in the accelerated tumor growth observed in vivo with ZA, we investigated the molecular and immunohistochemical expression of TRAP, RANK, and RANK involved in the differentiation and activation of osteoclasts, and of VEGF and CD146 as vascularization markers. We observed a non-significant decrease in *TRAP* mRNA expression in the animals treated with ZA using both human and murine primers (Figure 4a), while no difference was observed by immunohistochemistry of the same marker (immunoscore 1.50 ± 1.27 in the control group versus 1.4 ± 0.52 in the ZA group; $p = 0.90$) (Figure 5). Concerning the RANKL/RANK signaling molecules, a trend of increased mRNA expression was noted in the

ZA-treated group (Figure 4b,c), but the immunohistochemical analysis failed to reveal any difference between the two groups as a result of high background noise and low immunostaining (Figure 5). Finally, no significant difference was observed in VEGF expression between the animals treated with ZA or with placebo (Figure 4d). Moreover, there was no difference in the number of micro-vessels in the immunohistochemical study of CD146 (mean 149.4±42.8 vascular elements/mm^2 in the control group versus 149.3±72.1 elements/mm^2 in the ZA group, $p=0.75$) (Figure 5).

4 | DISCUSSION

The association between bone resorption and tumor growth has been demonstrated in LBO models (Heymann et al., 2004; Heymann, Fortun, et al., 2005), supporting the study of osteolysis inhibitors including bisphosphonates and in particular ZA in patients (Heymann et al., 2020). This study is the first to investigate the use of ZA in a JO model developed in immunodeficient mice. We found that there was a nonstatistically significant increase in the kinetics

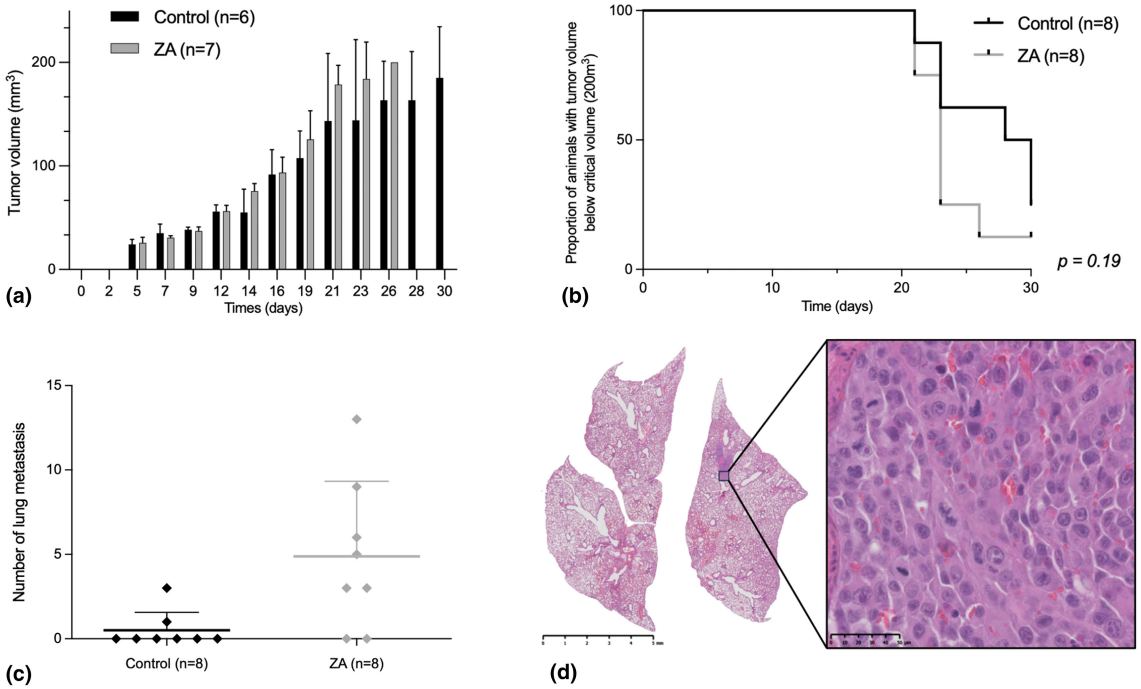

FIGURE 2 Clinical parameters of animals in the control and the zoledronic acid (ZA) groups. Comparative analysis of the mean mandibular tumor volume over time (a), Kaplan–Meier curves representing the proportion of animals with a tumor volume reaching the critical volume of 200 mm^3 (b). Comparison of the number of lung metastases between the control and the treated animals (c). Hematoxylin–eosin staining of a section of the lungs on an NMRI-nude mouse treated with ZA showing the presence of lung metastasis (left), and presenting as clusters of cells with large nuclei and abundant vascularization (original magnification (OM) 40×) (d).

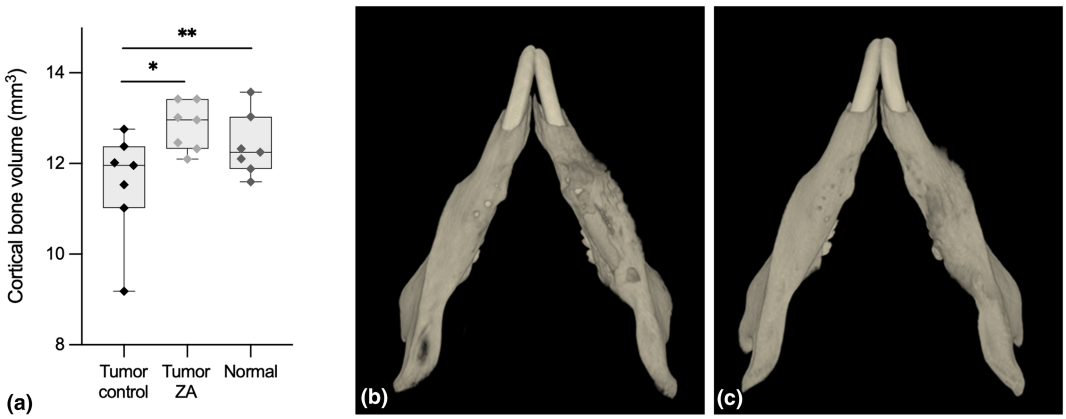

FIGURE 3 Comparison of the mean mandibular cortical volume around the tumor between the control and the zoledronic acid (ZA) groups, and in the normal contralateral side (*$p_1=0.01$, **$p_2=0.03$) (a). Three-dimensional reconstruction of the inferior jaw in an animal of the control group (b) and in an animal treated with ZA (c).

of tumor growth, as well as a significant increase in lung metastases, in the treated animals. These results contradict those obtained in most LBO models. In the immunocompetent OSRGa rat model, ZA reduced the tibia tumor growth and inhibited the tumor-associated osteolysis (Heymann, Ory, et al., 2005). In mice, high doses of ZA (100–120 μg/kg) administered subcutaneously twice a week inhibited tibia tumor growth and significantly reduced lung metastasis, while it improved survival in both immunocompetent (POS-1 cells in C3H/He mice) and immunodeficient (human SaOS2 in NMRI-nudes) models (Dass & Choong, 2007; Ory et al., 2005). Our results are more in line with those obtained by Labrinidis et al., who reported the use of subcutaneous injection of ZA (100 μg/kg, once a week or as a single dose) in a tibial model of osteosarcoma developed with human K-HOS cells (identical to HOS1544 cell lines) in BALB/c *nu/nu* mice (Labrinidis et al., 2009). The authors reported the absence of an effect of ZA on the tumor burden, and a trend of increased lung metastasis in treated animals (Labrinidis et al., 2009). The same authors reported the absence of effects of ZA on tumor growth and against pulmonary metastases in a rat model of osteosarcoma (MSK-8G) (Labrinidis et al., 2010).

In humans, two phase III trials did not demonstrate therapeutic benefit of combining ZA with conventional chemotherapy in LBO. The randomized controlled trial from the French consortium (OS2006) was prematurely discontinued due to local progression, metastasis, or relapse of disease in patients treated with bisphosphonate (Piperno-Neumann et al., 2016). The study by Li et al. (2019) performed with 798 patients, including 399 receiving ZA, found a decreased overall survival in the treated patients.

TABLE 2 Comparison of bone microarchitectural cortical and trabecular parameters between the group of control animals and the treated animals (ZA).

	Control	ZA	*p*-Value
Xenogenic HOS1544 model			
BV, mean ± SD (mm^3)	11.55 ± 1.18	12.81 ± 0.53	0.011
BV/TV, mean ± SD (%)	26.11 ± 5.25	25.93 ± 2.80	>0.99
Tb.Th, mean ± SD (mm)	0.15 ± 0.01	0.17 ± 0.01	0.001
Tb.Sp, mean ± SD (mm)	0.43 ± 0.01	0.50 ± 0.06	0.209
Tb.N, mean ± SD (mm^{-1})	1.74 ± 0.22	1.51 ± 0.17	0.018

Abbreviations: BV, bone volume; BV/TV, bone volume/total volume; Tb.N, trabecular number; Tb.Sp, trabecular separation; Tb.Th, trabecular thickness; ZA, zoledronic acid.

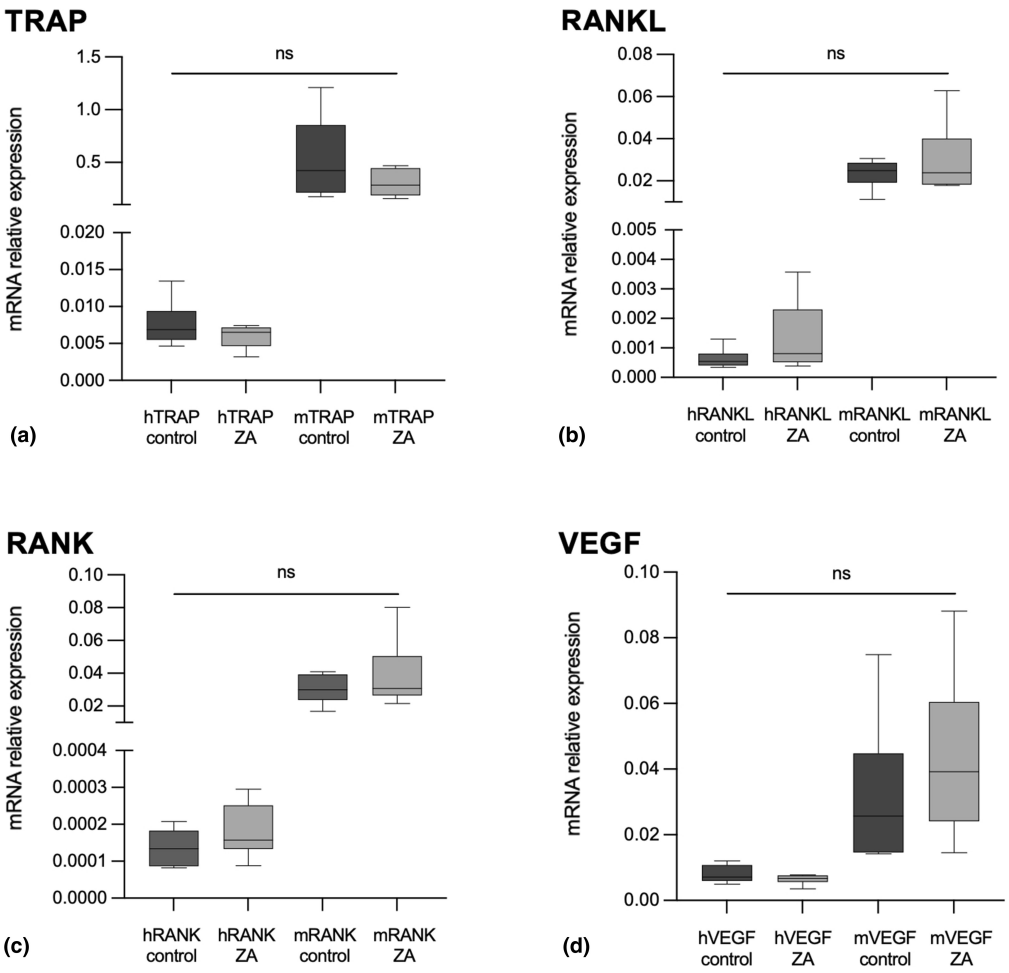

FIGURE 4 Real-time polymerase chain reaction (RT-PCR) molecular analysis of the osteoclastic marker *TRAP* (a), the bone remodeling markers *RANK* (b)/*RANK* (c), and the vascular markers *VEGF* (d).

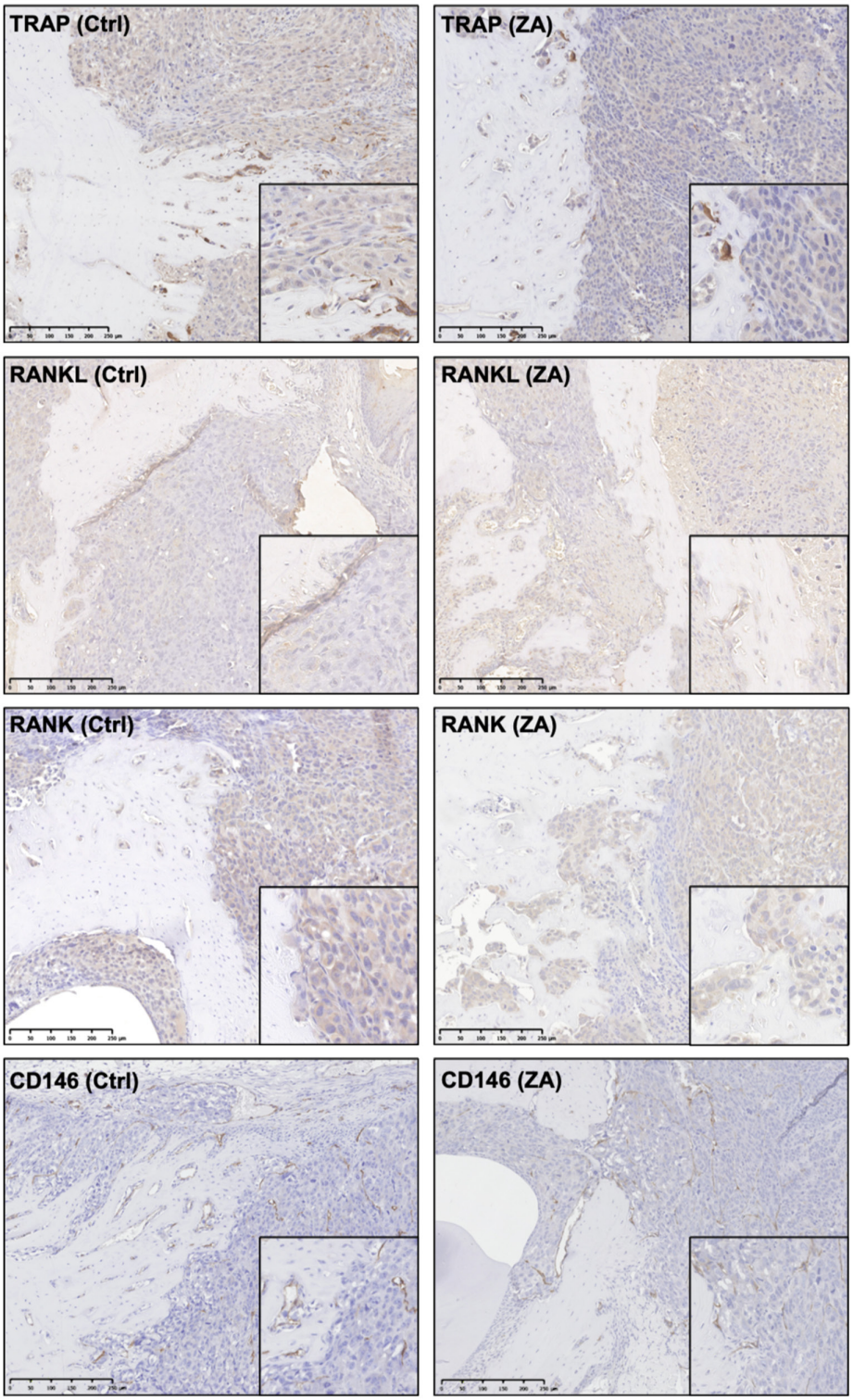

FIGURE 5 Immunohistochemical staining of the osteoclast (TRAP), bone remodeling (RANK/RANKL), and vascular (CD146) markers in JO samples in control (Ctrl) and ZA-treated animals (OM 10×, right window OM 40×).

There are several parameters that can explain the conflicting results observed in animal models and in human disease. First, the heterogeneity of the cell lines and animal models (xenogenic versus syngeneic) used for tumor induction as well as the use of different tumor inoculation protocols (orthotopic versus heterotopic, intraosseous versus paraosseous grafting) could account for the differences observed. In a previous study, we reported on the differences in the clinical behavior in terms of tumor growth, metastatic spread, and morphometric parameters of various xenogenic, syngeneic, and patient-derived xenograft (PDX) models of JO

(Bertin et al., 2019). Second, the rationale behind the use of bone antiresorptive therapy, whereas osteosarcoma is first and foremost a proliferation of osteoblasts that produce bone substance. Inhibiting osteolysis at the tumor site could, therefore, facilitate tumor growth and the production of osteoid substances. Data on the actual role of osteoclasts in tumor progression and metastatic dissemination are still unclear (Endo-Munoz et al., 2010; Heymann et al., 2020). It is possible that the osteoclastic environment of osteosarcomas may evolve towards an initial osteoclastogenesis favoring tumor growth in which bisphosphonates could be effective. Once the reduction in osteoclast activity has been obtained, there is a therapeutic escape, due to a switch toward tumor osteoformation (Endo-Munoz et al., 2012). In addition, JO is a separate entity from LBO, both clinically and in terms of disease pathophysiology (Bertin et al., 2020, 2023). The differences observed in animal models may, therefore, be partly explained by a distinct microenvironment depending on the tumor location. For JO, bone resorption inhibitors have not been tested in human disease; however, the present study appears to not support their use.

This study also explored the mandibular morphometric parameters in the tumor area. When injected in contact with bone, tumor cells induced tumor osteolysis, as evidenced by the significant reduction in mandibular cortical BV on the tumor side compared with the contralateral jaw in control animals. Such tumor-associated osteolysis has been observed in LBO xenogenic models induced with human HOS1544 cells (Bertin et al., 2019; Labrinidis et al., 2009). In contrast, the use of ZA prevented the osteolysis associated with the tumor, as evidenced by the increase in BVs in the treated animals. The "bone protective" effect of bisphosphonates has already been demonstrated in several models of LBO (Curtis et al., 2016; Labrinidis et al., 2009, 2010; Wolfe et al., 2011). However, it is unclear how ZA can promote both bone formation around the tumor and the tumor progression in the present model of JO. Labrinidis et al. suggested that ZA, by altering the spatial relationship and interaction of tumor cells with the bone stroma, could "force" cancer cells to escape the tumor niche and increase the metastatic spread (Labrinidis et al., 2009). However, there is currently no evidence of such an effect either in vivo or in vitro.

This study suggests that the effect of ZA is not mediated by osteoclasts, as both molecular and immunohistochemical analyses in treated animals did not reveal a significant decrease in the TRAP marker of osteoclast activity. ZA can directly interact with the tumor-associated macrophages (TAMs) (Junankar et al., 2015). Biteau et al. highlighted a synergic effect of ZA and L-mifamurtide (MEPACT®), an activator of macrophage populations, on tumor inhibition in two mouse models of LBO (Biteau et al., 2016). The immunohistochemical study performed on tumor samples from the OS2006 clinical series revealed a significant correlation between $CD163^+$ TAMs and survival in patients not treated with ZA (Gomez-Brouchet et al., 2017). The same authors reported inhibition of $CD68^+/CD163^-$ cells (corresponding to osteoclasts) and $CD68^-/CD163^+$ TAMs in tumor samples of patients receiving ZA (Gomez-Brouchet et al., 2021). In JO, $CD163^+$ TAMs may constitute a poor prognosis marker, as we previously demonstrated a strong correlation between CD163 staining and lower overall survival in an immunohistochemical study of 50 patients (Bertin et al., 2023). Moreover, the use of ZA was not associated with variations in tumor vascularization, as evidenced by the molecular study of VEGF, which mediates tumor angiogenesis in osteosarcoma (Kaya et al., 2000), and CD146, a biomarker of tumor vascularization (Wang et al., 2022). While the precise mode of action of bisphosphonates in tumor pathology has not been clearly established, various mechanisms have been proposed (Santini et al., 2003): alteration of the bone microenvironment, induction of tumor apoptosis, stimulation of γ/δ T cells and innate immune responses, and inhibition of tumor angiogenesis (Zekri et al., 2014). In particular, ZA has been shown to inhibit in vitro vascular mimicry of LM8 osteosarcoma cell lines (Fu et al., 2011) and reduced VEGF expression and secretion in a culture medium composed of non-small-cell lung cancer cells (Di Salvatore et al., 2011). Immunohistochemical studies in human JO disease found a lower degree of vascularization of JO tumors compared to LBO, and the absence of a correlation of vascularization of JO with clinical parameters and survival (Bertin et al., 2023; Jawad & Abdullah, 2010).

This study suffers from some limitations. The first lies in the use of a single model developed in immunodeficient animals, which prevents a full understanding of the immune mechanisms involved when using ZA. Furthermore, the rapid progression of tumors in the jaw localization imposed early sacrifice of the animals, thus preventing sufficiently long observation of the effect of treatments on survival. Nevertheless, the xenogenic model HOS1544 derives its advantage from the permanent and rapid development of lung metastasis (Biteau et al., 2016). The ZA effect could, therefore, be tested on the syngeneic mouse MOS-J model (Bertin et al., 2019). The use of a PDX model with orthotopic tumor grafting could overcome the aggressiveness of certain cell lines while preserving the "human" environment of the tumor. The second is the therapeutic study of ZA alone, that is, without any combination with chemotherapy, and, therefore, outside of normal clinical conditions of use. ZA in combination with ifosfamide has been found to be more effective than each agent used alone in preventing tumor recurrence in a rat model of LBO (Heymann, Fortun, et al., 2005). Suppression of chemoresistance in solid tumors is one of the mechanisms of action of ZA (Salaroglio et al., 2015). Finally, the molecular and immunohistochemical study should be extended to immune markers, in particular for macrophages (CD68 and CD163 staining), to investigate the mechanisms of action of ZA in JO models.

5 | CONCLUSION

The present study found increased tumor growth and metastatic spread in a mouse model of JO treated with ZA. While bisphosphonates have no place in the therapeutic strategy of LBO, their use in JO remains unexplored. It can be assumed that bisphosphonates may be beneficial for treating tumors with a large osteoclastic contingent,

provided the biopsy is sufficiently representative of the tumor environment. Nevertheless, further studies are needed to understand the role of bone resorption in the pathophysiology of JO.

AUTHOR CONTRIBUTIONS

Than-Thuy Nham: Conceptualization; investigation; writing – original draft; formal analysis; writing – review and editing. **Romain Guiho:** Conceptualization; investigation; methodology; writing – review and editing. **Régis Brion:** Formal analysis; writing – review and editing. **Jérôme Amiaud:** Formal analysis; writing – review and editing. **Bénédicte Brounais Le Royer:** Writing – review and editing; formal analysis. **Anne Gomez-Brouchet:** Writing – review and editing; validation; formal analysis. **Françoise Rédini:** Conceptualization; methodology; validation; writing – review and editing; supervision. **Hélios Bertin:** Supervision; writing – review and editing; writing – original draft; methodology; validation; conceptualization; formal analysis.

ACKNOWLEDGMENTS

This research was supported by the Fondation les Gueules Cassées (2018-51) and Nantes University Hospital. The sponsors had no role in the study design, the writing, or the submission of this manuscript.

CONFLICT OF INTEREST STATEMENT

The authors have no conflicts of interest to declare.

DATA AVAILABILITY STATEMENT

The data sets used and analyzed during the current study are available from the corresponding author upon reasonable request.

ORCID

Hélios Bertin https://orcid.org/0000-0002-0546-079X

REFERENCES

Alfranca, A., Martinez-Cruzado, L., Tornin, J., Abarrategi, A., Amaral, T., de Alava, E., Menendez, P., Garcia-Castro, J., & Rodriguez, R. (2015). Bone microenvironment signals in osteosarcoma development. *Cellular and Molecular Life Sciences*, *72*, 3097–3113.

Baumhoer, D., Brunner, P., Eppenberger-Castori, S., Smida, J., Nathrath, M., & Jundt, G. (2014). Osteosarcomas of the jaws differ from their peripheral counterparts and require a distinct treatment approach. Experiences from the DOESAK registry. *Oral Oncology*, *50*, 147–153.

Bertin, H., Gomez-Brouchet, A., & Rédini, F. (2020). Osteosarcoma of the jaws: An overview of the pathophysiological mechanisms. *Critical Reviews in Oncology/Hematology*, *156*, 103126.

Bertin, H., Guilho, R., Brion, R., Amiaud, J., Battaglia, S., Moreau, A., Brouchet-Gomez, A., Longis, J., Piot, B., Heymann, D., Corre, P., & Rédini, F. (2019). Jaw osteosarcoma models in mice: First description. *Journal of Translational Medicine*, *17*, 56.

Bertin, H., Peries, S., Amiaud, J., van Acker, N., Perrot, B., Bouvier, C., Aubert, S., Marie, B., Larousserie, F., de Pinieux, G., Crenn, V., Rédini, F., & Gomez-Brouchet, A. (2023). Characterization of the tumor microenvironment in jaw osteosarcomas, towards prognostic markers and new therapeutic targets. *Cancers (Basel)*, *15*, 1004.

Bialick, S., Campoverde, L., Gallegos, J. A. O., Barreto-Coelho, P., Watson, A., Arora, K., Perez, A., Lopez, E., Venkat, S., Rosenberg, A. E., Crawford, B., Jonczak, E., Trent, J., Dhir, A., & D'Amato, G. (2023). Osteogenic sarcoma of the head and neck: Is chemotherapy needed? *Current Treatment Options in Oncology*, *24*, 528–541.

Biteau, K., Guiho, R., Chatelais, M., Taurelle, J., Chesneau, J., Corradini, N., Heymann, D., & Redini, F. (2016). L-MTP-PE and zoledronic acid combination in osteosarcoma: Preclinical evidence of positive therapeutic combination for clinical transfer. *American Journal of Cancer Research*, *6*, 677–689.

Boon, E., van der Graaf, W. T. A., Gelderblom, H., Tesselaar, M. E. T., van Es, R. J. J., Oosting, S. F., de Bree, R., van Meerten, E., Hoeben, A., Smeele, L. E., Willems, S. M., Witjes, M. J. H., Buter, J., Baatenburg de Jong, R. J., Flucke, U. E., Peer, P. G. M., Bovée, J. V. M. G., & van Herpen, C. M. L. (2017). Impact of chemotherapy on the outcome of osteosarcoma of the head and neck in adults. *Head & Neck*, *39*, 140–146.

Boopathi, E., Birbe, R., Shoyele, S. A., Den, R. B., & Thangavel, C. (2022). Bone health Management in the Continuum of prostate cancer disease. *Cancers (Basel)*, *14*, 4305.

Bouaoud, J., Beinse, G., Epaillard, N., Amor-Sehlil, M., Bidault, F., Brocheriou, I., Hervé, G., Spano, J. P., Janot, F., Boudou-Rouquette, P., Benassarou, M., Schouman, T., Goudot, P., Malouf, G., Goldwasser, F., & Bertolus, C. (2019). Lack of efficacy of neoadjuvant chemotherapy in adult patients with maxillo-facial high-grade osteosarcomas: A French experience in two reference centers. *Oral Oncology*, *95*, 79–86.

Bouxsein, M. L., Boyd, S. K., Christiansen, B. A., Guldberg, R. E., Jepsen, K. J., & Müller, R. (2010). Guidelines for assessment of bone microstructure in rodents using micro-computed tomography. *Journal of Bone and Mineral Research*, *25*, 1468–1486.

Cappariello, A., & Rucci, N. (2019). Tumour-derived extracellular vesicles (EVs): A dangerous 'message in a bottle' for bone. *International Journal of Molecular Sciences*, *20*, 4805.

Crenn, V., Biteau, K., Amiaud, J., Dumars, C., Guiho, R., Vidal, L., Nail, L. L., Heymann, D., Moreau, A., Gouin, F., & Redini, F. (2017). Bone microenvironment has an influence on the histological response of osteosarcoma to chemotherapy: Retrospective analysis and preclinical modeling. *American Journal of Cancer Research*, *7*, 2333–2349.

Curtis, R. C., Custis, J. T., Ehrhart, N. P., Ehrhart, E. J., Condon, K. W., Gookin, S. E., & Donahue, S. W. (2016). Combination therapy with zoledronic acid and parathyroid hormone improves bone architecture and strength following a clinically-relevant dose of stereotactic radiation therapy for the local treatment of canine osteosarcoma in athymic rats. *PLoS One*, *11*, e0158005.

Dass, C. R., & Choong, P. F. M. (2007). Zoledronic acid inhibits osteosarcoma growth in an orthotopic model. *Molecular Cancer Therapeutics*, *6*, 3263–3270.

Di Salvatore, M., Orlandi, A., Bagalà, C., Quirino, M., Cassano, A., Astone, A., & Barone, C. (2011). Anti-tumour and anti-angiogenetic effects of zoledronic acid on human non-small-cell lung cancer cell line. *Cell Proliferation*, *44*, 139–146.

Endo-Munoz, L., Cumming, A., Rickwood, D., Wilson, D., Cueva, C., Ng, C., Strutton, G., Cassady, A. I., Evdokiou, A., Sommerville, S., Dickinson, I., Guminski, A., & Saunders, N. A. (2010). Loss of osteoclasts contributes to development of osteosarcoma pulmonary metastases. *Cancer Research*, *70*, 7063–7072.

Endo-Munoz, L., Evdokiou, A., & Saunders, N. A. (2012). The role of osteoclasts and tumour-associated macrophages in osteosarcoma metastasis. *Biochimica et Biophysica Acta*, *1826*, 434–442.

Fu, D., He, X., Yang, S., Xu, W., Lin, T., & Feng, X. (2011). Zoledronic acid inhibits vasculogenic mimicry in murine osteosarcoma cell line in vitro. *BMC Musculoskeletal Disorders*, *12*, 146.

Gomez-Brouchet, A., Gilhodes, J., Acker, N. V., Brion, R., Bouvier, C., Assemat, P., Gaspar, N., Aubert, S., Guinebretiere, J. M., Marie, B., Larousserie, F., Entz-Werlé, N., Pinieux, G., Mascard, E., Gouin, F., Brousset, P., Tabone, M. D., Jimenez, M., Le Deley, M. C., … Rédini, F. (2021). Characterization of macrophages and osteoclasts in the

osteosarcoma tumor microenvironment at diagnosis: New perspective for osteosarcoma treatment? *Cancers (Basel)*, *13*, 423.

Gomez-Brouchet, A., Illac, C., Gilhodes, J., Bouvier, C., Aubert, S., Guinebretiere, J. M., Marie, B., Larousserie, F., Entz-Werlé, N., de Pinieux, G., Filleron, T., Minard, V., Minville, V., Mascard, E., Gouin, F., Jimenez, M., Ledeley, M. C., Piperno-Neumann, S., Brugieres, L., & Rédini, F. (2017). CD163-positive tumor-associated macrophages and CD8-positive cytotoxic lymphocytes are powerful diagnostic markers for the therapeutic stratification of osteosarcoma patients: An immunohistochemical analysis of the biopsies fromthe French OS2006 phase 3 trial. *Oncoimmunology*, *6*, e1331193.

Gomez-Brouchet, A., Mascard, E., Siegfried, A., de Pinieux, G., Gaspar, N., Bouvier, C., Aubert, S., Marec-Bérard, P., Piperno-Neumann, S., Marie, B., Larousserie, F., Galant, C., Fiorenza, F., Anract, P., Sales de Gauzy, J., & Gouin, F. (2019). Assessment of resection margins in bone sarcoma treated by neoadjuvant chemotherapy: Literature review and guidelines of the bone group (GROUPOS) of the French sarcoma group and bone tumor study group (GSF-GETO/RESOS). *Orthopaedics & Traumatology, Surgery & Research*, *105*, 773–780.

Granowski-LeCornu, M., Chuang, S.-K., Kaban, L. B., & August, M. (2011). Osteosarcoma of the jaws: Factors influencing prognosis. *Journal of Oral and Maxillofacial Surgery*, *69*, 2368–2375.

Heymann, D., Fortun, Y., Rédini, F., & Padrines, M. (2005). Osteolytic bone diseases: Physiological analogues of bone resorption effectors as alternative therapeutic tools. *Drug Discovery Today*, *10*, 242–247.

Heymann, D., Ory, B., Blanchard, F., Heymann, M. F., Coipeau, P., Charrier, C., Couillaud, S., Thiery, J. P., Gouin, F., & Redini, F. (2005). Enhanced tumor regression and tissue repair when zoledronic acid is combined with ifosfamide in rat osteosarcoma. *Bone*, *37*, 74–86.

Heymann, D., Ory, B., Gouin, F., Green, J. R., & Rédini, F. (2004). Bisphosphonates: New therapeutic agents for the treatment of bone tumors. *Trends in Molecular Medicine*, *10*, 337–343.

Heymann, M.-F., Lézot, F., & Heymann, D. (2019). The contribution of immune infiltrates and the local microenvironment in the pathogenesis of osteosarcoma. *Cellular Immunology*, *343*, 103711.

Heymann, M.-F., Lezot, F., & Heymann, D. (2020). Bisphosphonates in common pediatric and adult bone sarcomas. *Bone*, *139*, 115523.

Ishikawa, T. (2023). Differences between zoledronic acid and denosumab for breast cancer treatment. *Journal of Bone and Mineral Metabolism*, *41*, 301–306.

Jawad, S. N., & Abdullah, B. H. (2010). Proliferative, apoptotic and angiogenic potentials in jaws and long bones osteosarcomas: A comparative immunohistochemical study. *Journal of Oral Pathology & Medicine*, *39*, 681–686.

Junankar, S., Shay, G., Jurczyluk, J., Ali, N., Down, J., Pocock, N., Parker, A., Nguyen, A., Sun, S., Kashemirov, B., McKenna, C. E., Croucher, P. I., Swarbrick, A., Weilbaecher, K., Phan, T. G., & Rogers, M. J. (2015). Real-time intravital imaging establishes tumor-associated macrophages as the extraskeletal target of bisphosphonate action in cancer. *Cancer Discovery*, *5*, 35–42.

Kaya, M., Wada, T., Akatsuka, T., Kawaguchi, S., Nagoya, S., Shindoh, M., Higashino, F., Mezawa, F., Okada, F., & Ishii, S. (2000). Vascular endothelial growth factor expression in untreated osteosarcoma is predictive of pulmonary metastasis and poor prognosis. *Clinical Cancer Research*, *6*, 572–577.

Khadembaschi, D., Jafri, M., Praveen, P., Parmar, S., & Breik, O. (2022). Does neoadjuvant chemotherapy provide a survival benefit in maxillofacial osteosarcoma: A systematic review and pooled analysis. *Oral Oncology*, *135*, 106133.

Kontio, R., Hagström, J., Lindholm, P., Böhling, T., Sampo, M., Mesimäki, K., Saarilahti, K., Koivunen, P., & Mäkitie, A. A. (2019). Craniomaxillofacial osteosarcoma – The role of surgical margins. *Journal of Cranio-Maxillo-Facial Surgery*, *47*, 922–925.

Krishnamurthy, A., & Palaniappan, R. (2018). Osteosarcomas of the head and neck region: A case series with a review of literature. *Journal of Maxillofacial and Oral Surgery*, *17*, 38–43.

Labrinidis, A., Hay, S., Liapis, V., Findlay, D. M., & Evdokiou, A. (2010). Zoledronic acid protects against osteosarcoma-induced bone destruction but lacks efficacy against pulmonary metastases in a syngeneic rat model. *International Journal of Cancer*, *127*, 345–354.

Labrinidis, A., Hay, S., Liapis, V., Ponomarev, V., Findlay, D. M., & Evdokiou, A. (2009). Zoledronic acid inhibits both the osteolytic and osteoblastic components of osteosarcoma lesions in a mouse model. *Clinical Cancer Research*, *15*, 3451–3461.

Lee, R. J., Arshi, A., Schwartz, H. C., & Christensen, R. E. (2015). Characteristics and prognostic factors of osteosarcoma of the jaws: A retrospective cohort study. *JAMA Otolaryngology. Head & Neck Surgery*, *141*, 470–477.

Li, H.-S., Lei, S.-Y., Li, J.-L., Xing, P. Y., Hao, X. Z., Xu, F., Xu, H. Y., & Wang, Y. (2022). Efficacy and safety of concomitant immunotherapy and denosumab in patients with advanced non-small cell lung cancer carrying bone metastases: A retrospective chart review. *Frontiers in Immunology*, *13*, 908436.

Li, S., Chen, P., Pei, Y., Zheng, K., Wang, W., Qiu, E., & Zhang, X. (2019). Addition of zoledronate to chemotherapy in patients with osteosarcoma treated with limb-sparing surgery: A phase III clinical trial. *Medical Science Monitor*, *25*, 1429–1438.

Marec-Berard, P., Laurence, V., Occean, B.-V., Ray-Coquard, I., Linassier, C., Corradini, N., Collard, O., Chaigneau, L., Cupissol, D., Kerbrat, P., Saada-Bouzid, E., Delcambre, C., Gouin, F., Guillemet, C., Jimenez, M., Lervat, C., Gaspar, N., le Deley, M. C., Brugieres, L., & Piperno-Neumann, S. (2020). Methotrexate-etoposide-Ifosfamide compared with doxorubicin-cisplatin-Ifosfamide chemotherapy in osteosarcoma treatment, patients aged 18-25 years. *Journal of Adolescent and Young Adult Oncology*, *9*, 172–182.

Mirabello, L., Zhu, B., Koster, R., Karlins, E., Dean, M., Yeager, M., Gianferante, M., Spector, L. G., Morton, L. M., Karyadi, D., Robison, L. L., Armstrong, G. T., Bhatia, S., Song, L., Pankratz, N., Pinheiro, M., Gastier-Foster, J. M., Gorlick, R., de Toledo, S. R. C., … Savage, S. A. (2020). Frequency of pathogenic germline variants in cancer-susceptibility genes in patients with osteosarcoma. *JAMA Oncology*, *6*, 724–734.

Navet, B., Ando, K., Vargas-Franco, J. W., Brion, R., Amiaud, J., Mori, K., Yagita, H., Mueller, C., Verrecchia, F., Dumars, C., Heymann, M. F., Heymann, D., & Lézot, F. (2018). The intrinsic and extrinsic implications of RANKL/RANK signaling in osteosarcoma: From tumor initiation to lung metastases. *Cancers (Basel)*, *10*, 398.

Nissanka, E. H., Amaratunge, E. A. P. D., & Tilakaratne, W. M. (2007). Clinicopathological analysis of osteosarcoma of jaw bones. *Oral Diseases*, *13*, 82–87.

Ory, B., Heymann, M.-F., Kamijo, A., Gouin, F., Heymann, D., & Redini, F. (2005). Zoledronic acid suppresses lung metastases and prolongs overall survival of osteosarcoma-bearing mice. *Cancer*, *104*, 2522–2529.

Percie du Sert, N., Hurst, V., Ahluwalia, A., Alam, S., Avey, M. T., Baker, M., Browne, W. J., Clark, A., Cuthill, I. C., Dirnagl, U., Emerson, M., Garner, P., Holgate, S. T., Howells, D. W., Karp, N. A., Lazic, S. E., Lidster, K., MacCallum, C. J., Macleod, M., … Würbel, H. (2020). The ARRIVE guidelines 2.0: Updated guidelines for reporting animal research. *BMJ Open Science*, *4*, e100115.

Piperno-Neumann, S., Le Deley, M.-C., Rédini, F., Pacquement, H., Marec-Bérard, P., Petit, P., Brisse, H., Lervat, C., Gentet, J. C., Entz-Werlé, N., Italiano, A., Corradini, N., Bompas, E., Penel, N., Tabone, M. D., Gomez-Brouchet, A., Guinebretière, J. M., Mascard, E., Gouin, F., … French Sarcoma Group (GSF-GETO). (2016). Zoledronate in combination with chemotherapy and surgery to treat osteosarcoma (OS2006): A randomised, multicentre, open-label, phase 3 trial. *The Lancet Oncology*, *17*, 1070–1080.

Piperno-Neumann, S., Ray-Coquard, I., Occean, B.-V., Laurence, V., Cupissol, D., Perrin, C., Penel, N., Bompas, E., Rios, M., le Cesne, A., Italiano, A., Anract, P., de Pinieux, G., Collard, O., Bertucci, F., Duffaud, F., le Deley, M. C., Delaye, J., Brugieres, L., & Blay, J. Y. (2020). Results of API-AI based regimen in osteosarcoma adult patients included in the French OS2006/Sarcome-09 study. *International Journal of Cancer*, *146*, 413–423.

Salaroglio, I. C., Campia, I., Kopecka, J., Gazzano, E., Orecchia, S., Ghigo, D., & Riganti, C. (2015). Zoledronic acid overcomes chemoresistance and immunosuppression of malignant mesothelioma. *Oncotarget*, *6*, 1128–1142.

Santini, D., Vincenzi, B., Dicuonzo, G., Avvisati, G., Massacesi, C., Battistoni, F., Gavasci, M., Rocci, L., Tirindelli, M. C., Altomare, V., Tocchini, M., Bonsignori, M., & Tonini, G. (2003). Zoledronic acid induces significant and long-lasting modifications of circulating angiogenic factors in cancer patients. *Clinical Cancer Research*, *9*, 2893–2897.

Schneider, C. A., Rasband, W. S., & Eliceiri, K. W. (2012). NIH image to ImageJ: 25 years of image analysis. *Nature Methods*, *9*, 671–675.

Scotlandi, K., Hattinger, C. M., Pellegrini, E., Gambarotti, M., & Serra, M. (2020). Genomics and therapeutic vulnerabilities of primary bone tumors. *Cell*, *9*, 968.

Seidensaal, K., Dostal, M., Liermann, J., Adeberg, S., Weykamp, F., Schmid, M. P., Freudlsperger, C., Hoffmann, J., Hompland, I., Herfarth, K., Debus, J., & Harrabi, S. B. (2022). Inoperable or incompletely resected craniofacial osteosarcoma treated by particle radiotherapy. *Frontiers in Oncology*, *12*, 927399.

Thariat, J., Julieron, M., Brouchet, A., Italiano, A., Schouman, T., Marcy, P. Y., Odin, G., Lacout, A., Dassonville, O., Peyrottes-Birstwisles, I., Miller, R., Thyss, A., & Isambert, N. (2012). Osteosarcomas of the mandible: Are they different from other tumor sites? *Critical Reviews in Oncology/Hematology*, *82*, 280–295.

Thariat, J., Schouman, T., Brouchet, A., Sarini, J., Miller, R. C., Reychler, H., Ray-Coquard, I., Italiano, A., Verite, C., Sohawon, S., Bompas, E., Dassonville, O., Salas, S., Aldabbagh, K., Maingon, P., de la MotteRouge, T., Kurtz, J. E., Usseglio, J., Kerbrat, P., … Julieron, M. (2013). Osteosarcomas of the mandible: Multidisciplinary management of a rare tumor of the young adult a cooperative study of the GSF-GETO, rare cancer network, GETTEC/REFCOR and SFCE. *Annals of Oncology*, *24*, 824–831.

van den Berg, H., & Merks, J. H. M. (2013). Incidence and grading of cranio-facial osteosarcomas. *International Journal of Oral and Maxillofacial Surgery*, *43*, 7–12.

Verrecchia, F., & Rédini, F. (2018). Transforming growth factor-β signaling plays a pivotal role in the interplay between osteosarcoma cells and their microenvironment. *Frontiers in Oncology*, *8*, 133.

Wang, J., Wu, Z., Zheng, M., Yu, S., Zhang, X., & Xu, X. (2022). CD146 is closely associated with the prognosis and molecular features of osteosarcoma: Guidance for personalized clinical treatment. *Frontiers in Genetics*, *13*, 1025306.

Weber, V., Stigler, R., Lutz, R., Kesting, M., & Weber, M. (2023). Systematic review of craniofacial osteosarcoma regarding different clinical, therapeutic and prognostic parameters. *Frontiers in Oncology*, *13*, 1006622.

Wolfe, T. D., Pillai, S. P. S., Hildreth, B. E., Lanigan, L. G., Martin, C. K., Werbeck, J. L., & Rosol, T. J. (2011). Effect of zoledronic acid and amputation on bone invasion and lung metastasis of canine osteosarcoma in nude mice. *Clinical & Experimental Metastasis*, *28*, 377–389.

Wu, T., & Dai, Y. (2017). Tumor microenvironment and therapeutic response. *Cancer Letters*, *387*, 61–68.

Yu, L., Zhang, J., & Li, Y. (2022). Effects of microenvironment in osteosarcoma on chemoresistance and the promise of immunotherapy as an osteosarcoma therapeutic modality. *Frontiers in Immunology*, *13*, 871076.

Zekri, J., Mansour, M., & Karim, S. M. (2014). The anti-tumour effects of zoledronic acid. *Journal of Bone Oncology*, *3*, 25–35.

Zhu, T., Han, J., Yang, L., Cai, Z., Sun, W., Hua, Y., & Xu, J. (2022). Immune microenvironment in osteosarcoma: Components, therapeutic strategies and clinical applications. *Frontiers in Immunology*, *13*, 907550.

SUPPORTING INFORMATION

Additional supporting information can be found online in the Supporting Information section at the end of this article.

How to cite this article: Nham, T.-T., Guiho, R., Brion, R., Amiaud, J., Le Royer, B. B., Gomez-Brouchet, A., Rédini, F., & Bertin, H. (2024). Zoledronic acid enhances tumor growth and metastatic spread in a mouse model of jaw osteosarcoma. *Oral Diseases*, *30*, 4209–4219. https://doi.org/10.1111/odi.14897